NORSAR

ROYAL NORWEGIAN COUNCIL FOR SCIENTIFIC AND INDUSTRIAL RESEARCH

Scientific Report No. 2 - 81/82

SEMIANNUAL TECHNICAL SUMMARY

1 October 1981—31 March 1982

By
Jørgen Torstveit (ed.)

Kjeller, July 1982

Sponsored by
Advanced Research Projects Agency
ARPA Order No. 2551

VI.6 A North Sea - Southern Norway seismic crustal profile

Introduction

During the last decade numerous seismic profiling investigations have been carried out in Fennoscandia and a relatively large number of crustal models have been derived. There is considerable inconsistency concerning the number of crustal layers and the associated velocity distributions as reported by various authors. The reason for this is probably a combination of real crustal variations, relatively poor sampling densities and the non-uniqueness inherent in the interpretation of refraction seismic data. Consequently, as a Cambridge group was carrying out a refraction experiment across the North Sea in the summer of 1980, we took the opportunity to expand the shot-firing scheme in order to obtain a densely sampled land profile (CANOBE) in southern Norway. The profile was positioned in a north-easterly direction, away from the line of shots off the southern coast and running parallel to the western border of the Oslo Graben as shown in Fig. VI.6.1.

In this section we present an interpretation of the high quality records obtained along the densely sampled CANOBE profile. Synthesis of P-wave amplitudes and travel times, assuming a laterally varying structure, constitutes the basic tool for mapping the crustal structure and thickness in the coastal areas of southern Norway and the general features of the Moho near and in the Oslo Graben.

Field work and preparation of the data

The CANOBE project, its name derived from the participating institutions Cambridge University, NORSAR and Bergen University, took place between the 26th of July and the 4th of August 1980. A total of 13 recording instruments were available. Four explosions from a coinciding Cambridge North Sea refraction project (N2-N5 in Fig. VI.6.1) were located to the east of the Central Graben in the North Sea, and were used for the land-recording in Norway. In addition the Royal Norwegian Navy provided several tons of AMATOL in the form of torpedo warheads and a coast guard ship to fire shots H1-H6 also marked in Fig. VI.6.1.

The recording scheme consisted of seven legs (Fig. VI.6.1), one per shot, each comprising 13 mobile stations. Legs 1 to 3 had a sensor spacing of 4 km, legs 4 to 6 a 6 km spacing and leg 7 a spacing of 5 km. Leg 7 transected the Oslo Graben just north of Oslo while the main line ran across the Precambrian rocks to the west, extending into the NORSAR array siting area. Five NORSAR subarrays (01A, 02C, 03C, 04C, 06C) recorded the shots continuously, thus enabling the main line distance range to be extended to about 515 km.

The initial record sections were filtered between 0.2 and 15 Hz. Fig. VI.6.2 shows the record section corresponding to the main line for shots N5 and H1-H5, reduced by 8 km/s. The NORSAR array records, from 450 km onwards, have been low pass filtered at 4.75 Hz sampling rate 20 Hz. True amplitudes are multiplied by distance in the record sections. The spectra for typical records in this section are found to have dominant frequencies within 2.5 to 3.5 Hz.

Interpretation of the CANOBE data

Although the quality of the data and the relatively dense sensor spacing along the profile provide and excellent basis for interpretation we are somewhat encumbered by lack of observations for the first 70 km of the profile and by the absence of a reversed coverage. This being said, the interpretational results are as follows:

Interpretation of the main line section assuming lateral homogeneity

Starting with P_g and P_n velocities taken from the record section (Fig. VI.6.2) and Moho depths in the expected range of 30-35 km, theoretical time-distance curves were computed until a satisfactory fit with the data was achieved. A prominent feature in the record section are the large amplitudes of secondary arrivals at about 186 km, apparently part of the P_MP branch. While modelling the data on the basis of travel times a velocity-depth configuration was established which produces a focusing effect near the outer cusp in the triplication (Fig. VI.6.3). The outer cusp is made to terminate at 250 km by introducing a velocity gradient of 0.025 s^{-1} in the depth interval 5.5 km to 25 km, and an increasing velocity gradient

down to 32.5 km where a velocity of 8.1 km/s is reached. As can be seen in the figure, the computed subcritical reflection travel times do not agree with the secondary arrivals between 70 km and 110 km.

Now, applying the reflectivity method to the model in Fig. VI.6.3, the above gradient is sufficient to reproduce large amplitudes in the retrograde travel-time branch of the observations (Fig. VI.6.4). The theoretical amplitudes near the critical distance are large in comparison with the observed ones. However, further attempts to model these amplitudes in the context of laterally homogeneous models were not considered due to the mentioned travel time discrepancies.

Interpretation of the main line section assuming a laterally varying structure

From the results of previous profiling experiments and seismological studies in southern Norway (Fig. VI.6.1) crustal structure and Moho depth are expected to vary especially around the endpoints of the CANOBE profile. It is essential at this stage to deduce a model for the first 200 km of the profile for which P_MP observations are available in addition to the Pg and Pn phases. Close examination of Fig. VI.6.5 reveals that strong P_MP amplitudes are confined to two distinct distance intervals. The first is around 115 km and is considered to be near the critical distance where relatively large amplitudes are expected. The second is around 185 km and is limited to a few seismograms. The latter extreme P_MP-amplitudes can be attributed to focusing effects caused by waves touching a caustic. While modelling these large amplitudes, however, the relatively early P_MP subcritical arrivals (Fig. VI.6.3) must be accounted for. These suggest a thinner crust as compared to the laterally homogeneous model of the previous section although the travel-times of the P_n arrivals from 150 km onwards must still be retained.

The calculations for the laterally varying models are performed using Cassell's (1982) box method (based on zero-order ray theory) where physical medium parameters are defined at 1 x 1 km grid points. A model is presented in Fig. VI.6.6 which produces good agreement between the theoretical and

observed travel times. The main features in the model consist of a Moho with a depth of 26 to 28 km off-coast which increases to 33 km over a distance of 30 km beneath the coastline. The velocity gradient directly above the Moho is similar to that in Fig. VI.6.3 except that it does not follow the topography of the Moho from 80 km onwards but remains at a constant depth and gradually fades away after 200 km as shown in Fig. VI.6.8. In the coastal area the main discontinuity, associated with a velocity jump from 6.8 to 7.5 km/s, occurs at a depth of 26-28 km and is overlying a velocity gradient zone reaching a velocity of 8.1 km/s at 34 km. In this region the Moho should be regarded as a transition zone in which its depth is not clearly defined. Beyond 110 km the Moho materializes into a first order discontinuity with a P_n velocity of 8.1 km/s. The upper mantle velocity gradient is approximately 0.008 s^{-1}.

Synthetic seismograms were calculated for Model 1 (Fig. VI.6.7). Note that zero-order ray theory as used here is not exact near caustics or crictical points. Nevertheless, the amplitude distribution in the synthetic section qualitatively justifies the choice of the model. The amplitude distribution exhibits distinct peaks corresponding to the critical point of the P_MP travel time branch and the caustic. The first theoretical amplitude maximum is located at 95 km whereas the observed maximum is found to be at approximately 115 km. This discrepancy is not surprising as zero-order ray theory does not include wave effects in the critical region beyond the critical point. A similar phenomenon applies to the amplitudes near the caustic, which are exaggerated by zero-order ray theory.

The P_n arrivals begin to undulate at distances greater than 270 km. The interpretation of structures in this distance range is ambiguous as we cannot determine whether the travel time perturbations are caused by Moho topography or by lateral crustal variations or a combination of both.

In Fig. VI.6.8 two possible structural configurations are presented which satisfy the P_n travel time data. The modelling was done with the criterion

of fitting computed travel time curves to the trend of the two apparent velocities in the P_n arrivals. These are a model with a varying Moho (Model 1) and one with a varying surface layer thickness (Model 2).

Significant constraints are imposed on the interpretation when attempting to account for the late arrivals which occur between 16 and 20 s in the last 150 km of the main line. These arrivals appear to be surface multiples corresponding to the P_g, P_MP and P_n phases of the first arrivals. When calculating multiple ray paths for Model 1, we find that the corresponding travel times fall approximately 1 second short of the observed arrivals. This indicates that the mean crustal velocity is too high as these waves travel only in the crust. The required delay is achieved for Model 2 in Fig. VI.6.8 by introducing a Moho depth of 30 km and a mean crustal velocity of 6.16 km/s.

In Fig. VI.6.9 synthetic seismograms are calculated for Model 2. The increasing P_n amplitudes with distance are in general agreement with those in the observations, although the theoretical ones are not continuous throughout all the records. This inconsistency is caused by unavoidable lateral velocity gradients in the laterally varying model. The multiple arrivals, however, have much smaller relative amplitudes than those in the observations. In a few cases, some of the theoretical records lack arrivals due to difficulties in finding rays to each receiver location.

Discussion and Conclusions

In this study we have demonstrated that the use of amplitude information as a supplement to travel time data is essential in delineating earth structure. The outstanding example here is the extremely strong amplitudes in the P_MP branch, confined to a relatively small distance interval around 180 km, which appears to be created by a strong velocity gradient in the lower crust. In this respect, the calculations of amplitudes for 2-D media proved very important as compared to the 1-D amplitude calculations by the reflectivity method.

The Moho is found to be 27 to 28 km deep beneath the first 80 km of the profile before it dips downward over a distance of 30 km beneath the coast and subsequently levels out at a depth of approximately 34 km. The interpretation of the record section presented is only approximate for the last 300 km of the main line. Two structural models were proposed for this distance range. In order to keep the results presented here consistent with Kongsberg seismograph station data (Bungum et al (1980) find a Moho depth of 34 km at Kongsberg - see Fig. VI.6.1), preference should be given to Model 1 in Fig. VI.6.8. In this model the Moho becomes slightly shallower as it approaches the margin of the Oslo Graben from the southwest. After a distance of 310 km along the profile it appears to sink to 36 km from where it, over a distance of 180 km, rises to a depth of approximately 35 km beneath the NORSAR array. This Moho depth is in general agreement with Berteussen's (1977) Moho depth values which are based on spectral ratio analysis of long period P waves recorded at NORSAR.

On the other hand, Model 2 of Fig. VI.6.8 resulted from an attempt to correlate the strong secondary arrivals in the last 100 km of the profile, interpreted as multiple surface reflections of the P_g, P_MP and P_n phases. The travel time delays in the crust, which are required for the correlation of these multiple phases, infer a decrease in mean crustal velocity by as much as 0.3 km/s and an elevation of the Moho by 5 km in comparison with Model 1. Still, the synthetic section (Fig. VI.6.9) for Model 2 was not particularly successful in matching the amplitudes of multiple phases, and the possibility remains that the phases in question have not been correctly identified. So, in order to conform with previous investigations, we adopt Model 1 as representative for the main profile.

S. Mykkeltveit
E.S. Husebye
B. Cassell (Univ. of Cambridge, UK)
R. Kanestrøm (Univ. of Bergen)

References

Berteussen, K.-A., 1977: Moho depth determinations based on spectral ratio analysis of NORSAR long period P-waves. Phys. Earth Planet. Int., 15, 13-27.

Bungum, H., S.E. Pirhonen and E.S. Husebye, 1980: Crustal thicknesses in Fennoscandia. Geophys. J.R. astr. Soc., 53, 759-774.

Cassell, B.R., 1982: A method for calculating synthetic seismograms in laterally varying media. Geophys. J.R. astr. Soc., 69, 339-355.

Kanestrøm, R. and K. Haugland, 1971: Profile section 3-4, In: Deep Seismic Sounding in Northern Europe, A. Vogel (ed.), Swedish Natural Science Research Council, Stockholm, 76-91.

Kanestrøm, R. and S. Nedland, 1975: Crustal structure of southern Norway: A reinterpretation of the 1965 Seismic Experiment. Publication No. 117 in the Norwegian Geotraverse Project. In: Seismic Investigations of the Crust and Moho in Southern Norway, R. Kanestrøm (ed.), Univ. of Bergen, Seismological Observatory.

Mykkeltveit, S., 1980: A seismic profile in southern Norway. Pure and Appl. Geophys., 118, 1310-1325.

Sellevoll, M.A. and R.E. Warrick, 1971: A refraction study of the crustal structure of southern Norway.

Tryti, J. and M.A. Sellevoll, 1977: Seismic crustal study of the Oslo Rift. Pure and Appl. Geophys., 115, 1061-1085.

Weigel, W., J. Hjelme and M.A. Sellevoll, 1970: A refraction profile through the Skagerrak from northern Jutland to Southern Norway. Geodætisk Inst., Meddelelse No. 45, 1-28.

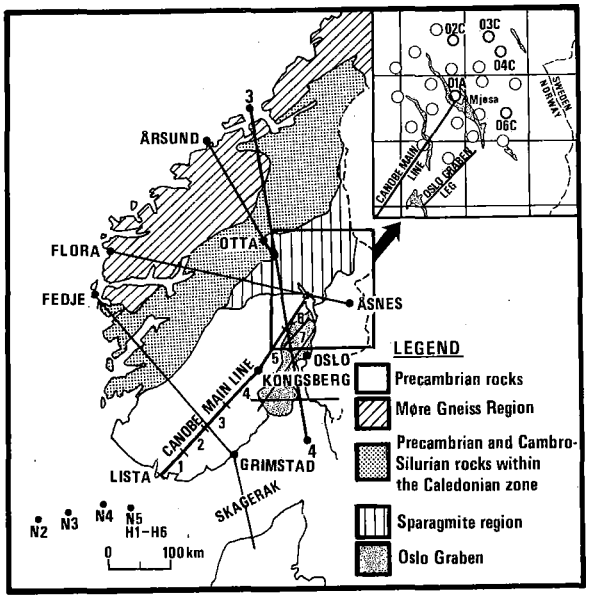

Fig. VI.6.1 Simplified geological map of southern Norway with CANOBE shot points and recording legs. Results from previous profiles are reported by Sellevoll & Warrick (1971) and Kanestrøm & Nedland (1975) for the Flora-Åsnes and Fedje-Grimstad profiles, Kanestrøm & Haugland (1971) for the '3-4'-profile, Tryti & Sellevoll (1977) for profiles in the Oslo Graben, Weigel et al (1970) for the Skagerrak profile and Mykkeltveit (1980) for the Årsund-Otta profile. Also shown is the NORSAR array siting area with the original 22 subarrays, each comprising 6 short period instruments. Five of the subarrays (bold rings) recorded the CANOBE shots.

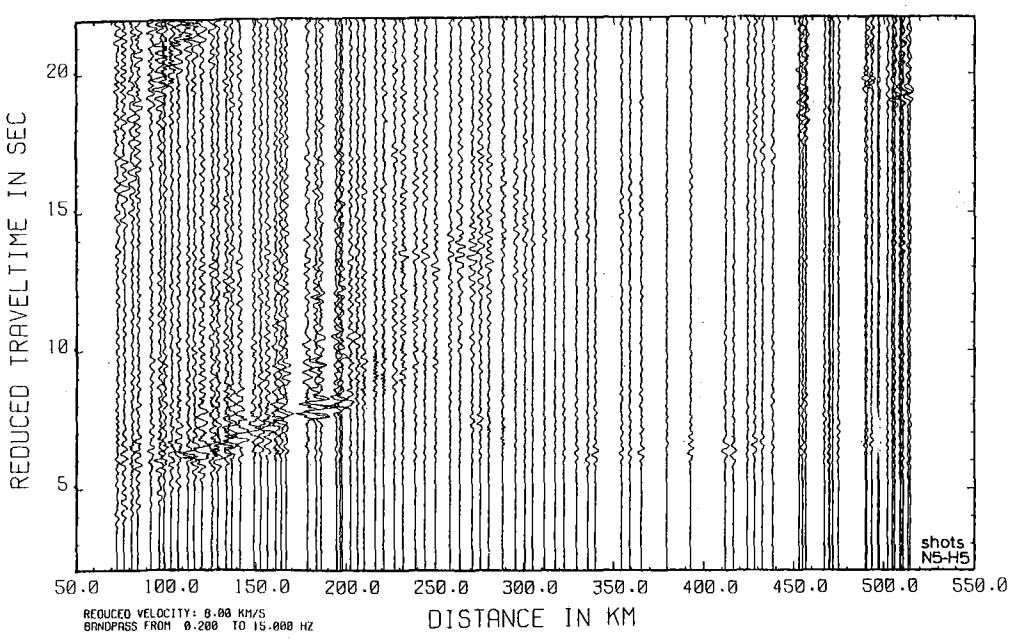

Fig. VI.6.2 Main line record section. Amplitudes are multiplied by distance and the seismograms are filtered between 0.2 and 15 Hz. The records beyond 450 km were recorded by the NORSAR array. The continuation of the crustal phase to the origin is not clear although an intercept time of 1.1 s indicates a travel time delay in the upper crust.

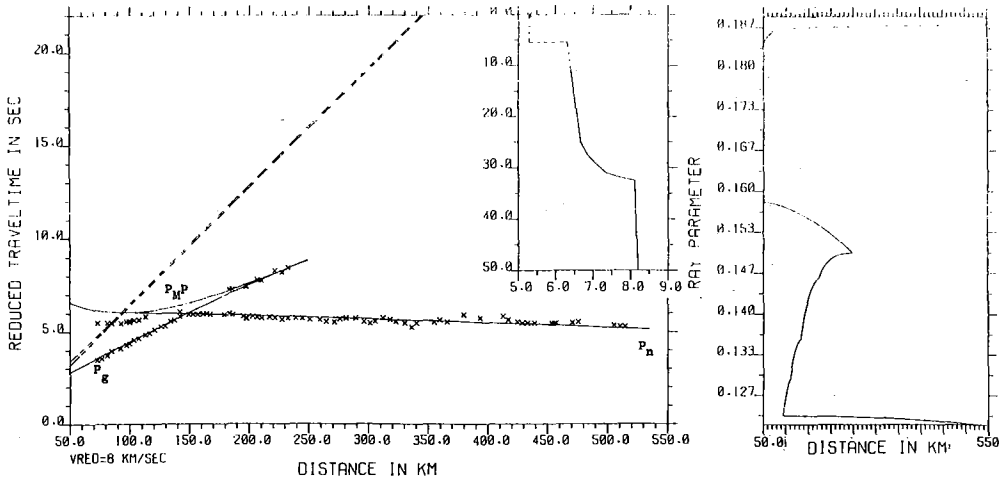

Fig. VI.6.3 Travel time-distance curves for the laterally homogeneous velocity-depth model (inserted). The portion of the velocity-depth function corresponding to unrecorded arrivals in the first 70 km of the record section is dashed. Crosses indicate observed arrivals. Note the discrepancy between observed and theoretical subcritical P_MP which indicates an elevated Moho beneath the first part of the profile.

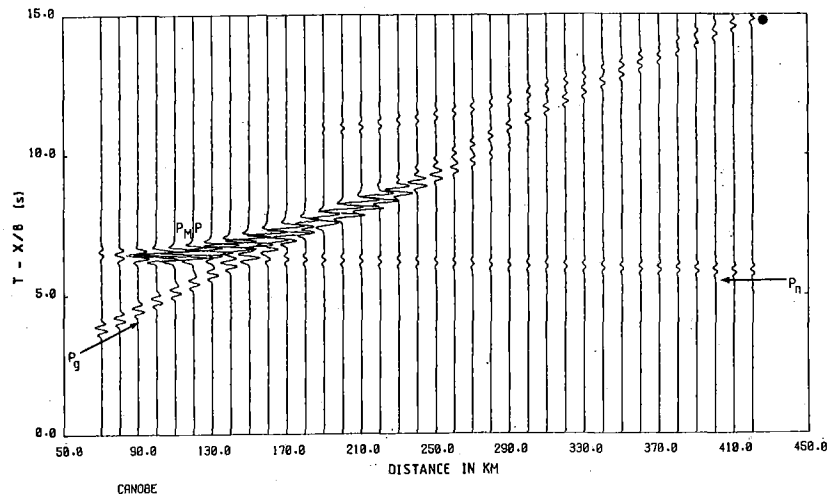

Fig. VI.6.4 Synthetic seismograms computed by the reflectivity method for the model in Fig. VI.6.3. The source signal has a dominant frequency of 3 Hz and 4 extrema. The dot indicates the outer cusp in the P_MP-surface layer multiple caused by the artificial first order discontinuity. The strong P_MP amplitudes are produced by the velocity gradient in the crust. Amplitudes are multiplied by distance.

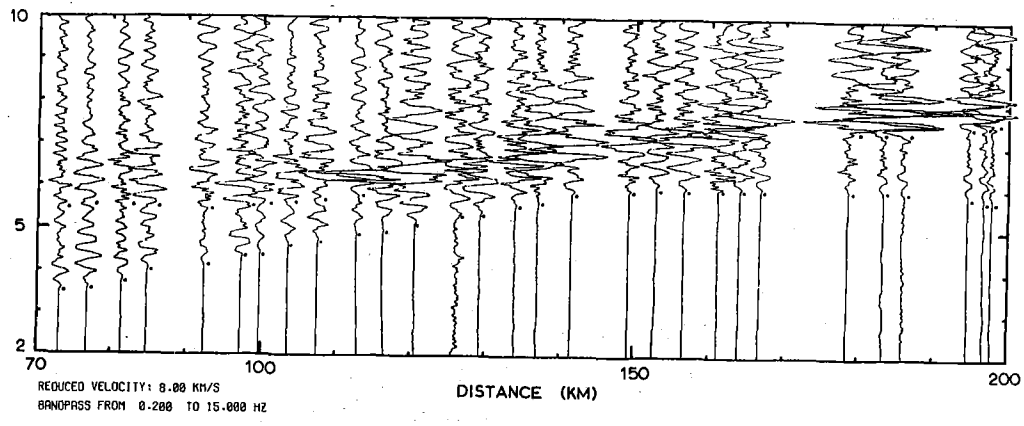

Fig. VI.6.5 Arrival picks in the main line record section. Amplitude maxima in the secondary arrivals occur at 115 and 185 km.

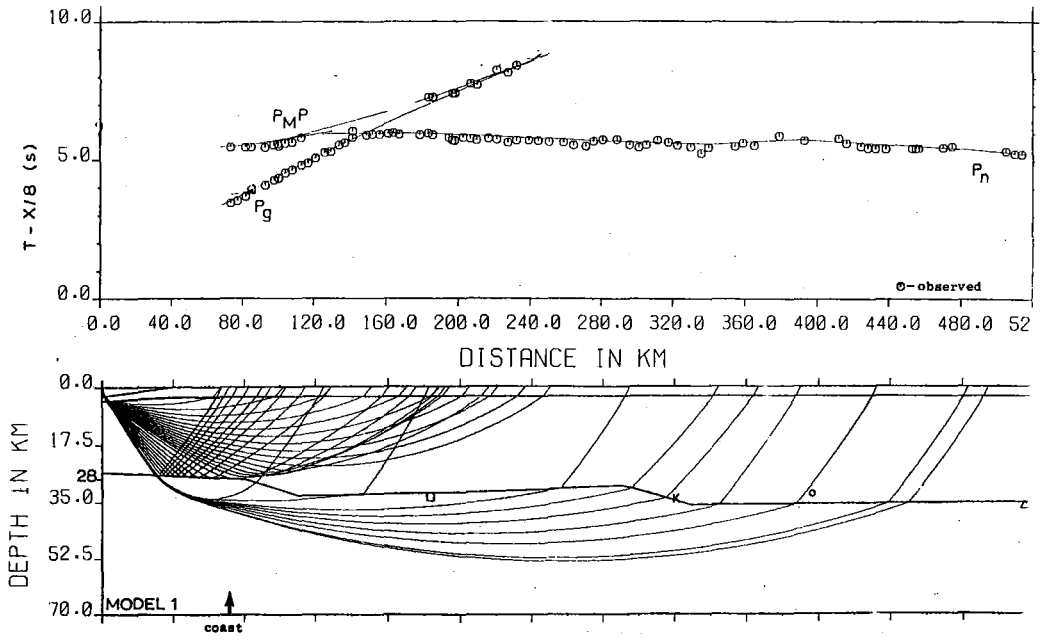

Fig. VI.6.6 Comparison of observed travel times and theoretical ones computed for Model 1 in Fig. VI.6.8. The vertical radii of the symbols indicating the observed times represent the reading errors. K denotes the Moho depth derived from Kongsberg seismograph station data. (Bungum et al, 1980)

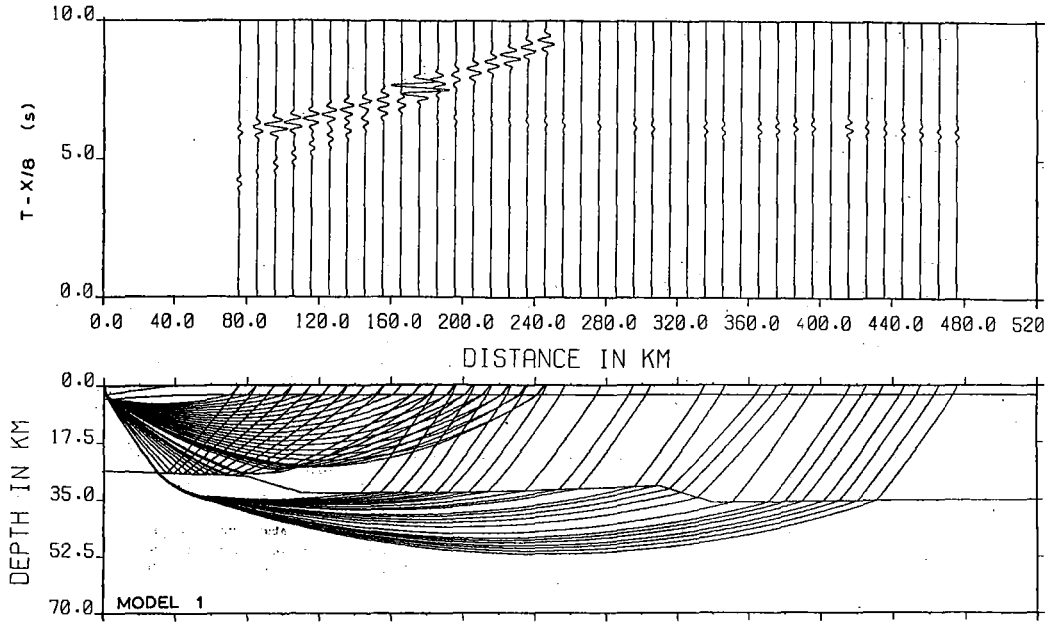

Fig. VI.6.7 Synthetic seismograms for the box method (Cassell, 1982). The source wavelet has a dominant frequency of 3.1 Hz, and amplitudes are multiplied by distance. Note the large amplitude at 176 km resulting from the velocity gradient in the lower crust.

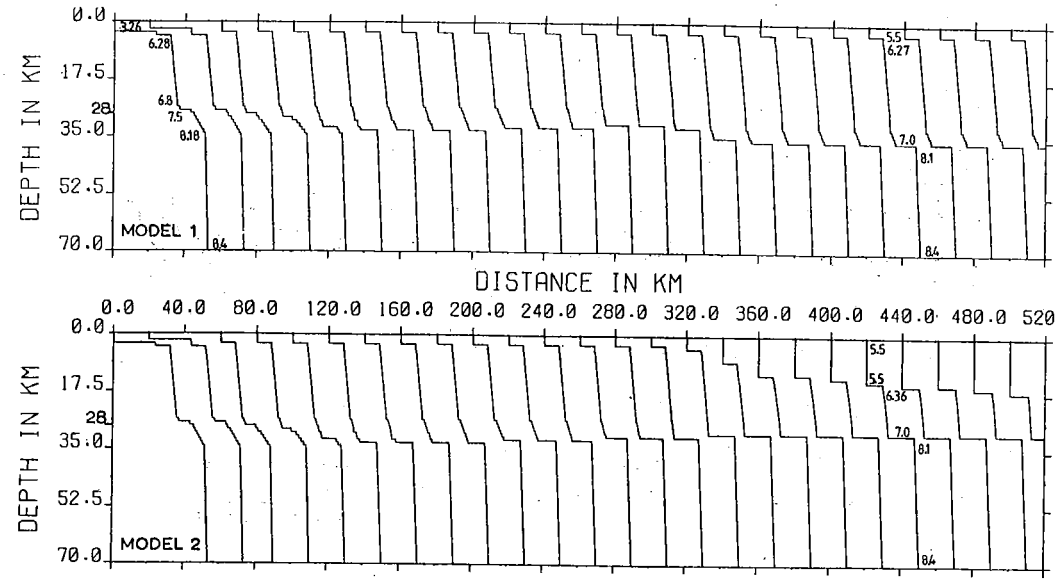

Fig. VI.6.8 Velocity-depth distributions for Models 1 and 2. The first order discontinuity in the crust after 340 km for Model 2 has not been observed and serves only to signify a decrease in the mean crustal velocity in that area.

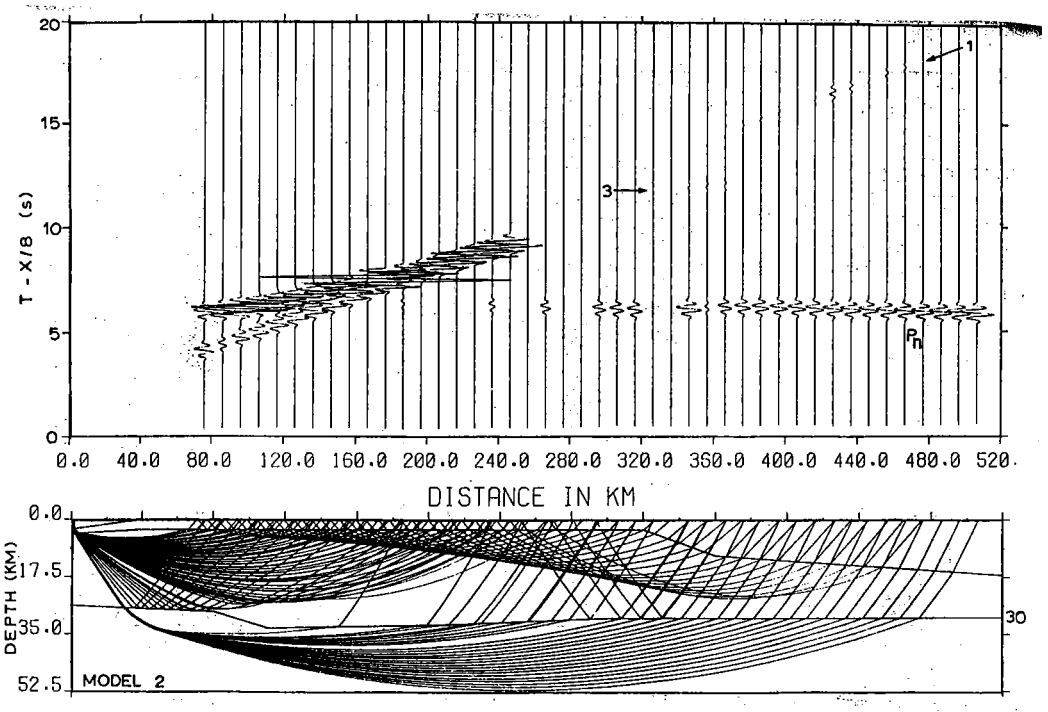

Fig. VI.6.9 Ray paths and synthetic seismograms for Model 2 in Fig. VI.6.8. The multiple arrivals '1' and '3' have smaller amplitudes than the corresponding observed phases.